J|A|C|S
ARTICLES
Published on Web 04/04/2006

Characterization of Weak NH$-\pi$ Intermolecular Interactions of Ammonia with Various Substituted π-Systems

Sascha Vaupel,[†] Bernhard Brutschy,*[,†] Pilarisetty Tarakeshwar,*[,‡] and Kwang S. Kim[§]

Contribution from the Institut für Physikalische und Theoretische Chemie, J. W. Goethe-Universität Frankfurt, Marie-Curie-Str. 11, D-60439 Frankfurt/Main, Germany, School of Computational Sciences, Korea Institute for Advanced Study (KIAS), 207-43 Cheongnyangni 2-dong, Dongdaemun-gu, Seoul 130-722, Korea, and National Creative Research Initiative Center for Superfunctional Materials, Department of Chemistry, Pohang University of Science and Technology, San 31, Hyojadong, Pohang 790-784, Korea

Received October 4, 2005; E-mail: brutschy@chemie.uni-frankfurt.de; tara@kias.re.kr

Abstract: Among the several weak intermolecular interactions pervading chemistry and biology, the NH$-\pi$ interaction is one of the most widely known. Nevertheless its weak nature makes it one of the most poorly understood and characterized interactions. The present study details the results obtained on gas-phase complexes of ammonia with various substituted π systems using both laser vibrational spectroscopy and ab initio calculations. The spectroscopic measurements carried out by applying one-color resonant two-photon ionization (R2PI) and IR-vibrational predissociation spectroscopy in the region of the NH stretches yield the first experimental NH stretching shifts of ammonia upon its interaction with various kinds of π-systems. The experiments were complemented by ab initio calculations and energy decompositions, carried out at the second-order Møller−Plesset (MP2) level of theory. The observed complexes show characteristic vibrational spectra which are very similar to the calculated ones, thereby allowing an in-depth analysis of the interaction forces and energies. The interaction energy of the conformers responsible for the observed vibrational spectra has the maximum contribution from dispersion energies. This implies that polarizabilities of the π-electron systems play a very important role in governing the nature and geometry of the NH$-\pi$ interaction. The larger polarizability of ammonia as compared to water and the tendency to maximize the dispersion energy implies that the characteristics of the NH$-\pi$ interactions are markedly different from that of the corresponding OH$-\pi$ interactions.

Introduction

There has been a tremendous interest to obtain information on the nature of weak intermolecular interactions because they govern the chemical and physical properties of molecular systems in the condensed phase.[1,2] Gas-phase complexes of molecules are useful in this context, because they serve as model systems to investigate isolated intermolecular interactions. Among the large number of available experimental methods, high resolution laser spectroscopic studies of molecular complexes produced under ultracold conditions in a supersonic jet expansion are particularly useful because they enable a systematic size and isomer specific investigation of the modulation of intermolecular interactions.[2,3−13] Apart from providing accurate insights into the structure and dynamics of these molecular complexes, they also help to develop, validate, and refine the theoretical models and approximations employed to characterize these complexes.[2,14] The benefits of such theoretical models in crystal and material design are well documented.[15,16]

[†] J. W. Goethe-Universität Frankfurt.
[‡] Korea Institute for Advanced Study (KIAS).
[§] Pohang University of Science and Technology.

(1) (a) Haberland, H. *Clusters of Atoms and Molecules*; Springer-Verlag: Berlin, 1994. (b) Haberland, H. In *Clusters, or the Transition from Molecular to Condensed Matter Physics*; Briggs, J. S., Kleinpoppen, H., Lutz, H. O., Eds.; NATO Advanced Study Institutes Series, D; Reidel Publishing Company: Dordrecht, Holland, 1988; Vol. B181, p 603. (c) Bartell, L. S. *Annu. Rev. Phys. Chem.* **1998**, *49*, 43. (d) Desiraju, G. R. *Nature* **2001**, *412*, 397.
(2) Brutschy, B. *Chem. Rev.* **1992**, *92*, 1567. Brutschy, B. *Chem. Rev.* **2000**, *100*, 3891.
(3) Bernstein, E. R. *Chemical Reactions in Clusters*; Oxford University Press: New York, 1996.
(4) Müller-Dethlefs, K.; Hobza, P. *Chem. Rev.* **2000**, *100*, 143.
(5) Zwier, T. S. *Annu. Rev. Phys. Chem.* **1996**, *47*, 205.
(6) Mons, M.; Dimicoli, I.; Piuzzi, F. *Int. Rev. Phys. Chem.* **2002**, *21*, 101.
(7) Simons, J. P. *Comptes Rendus Chimie* **2003**, *6*, 17. Snoek, L. C.; van Mourik, T.; Çarçabal, P.; Simons, J. P. *Phys. Chem. Chem. Phys.* **2003**, *5*, 4519.
(8) Mewly, M.; Bach, A.; Leutwyler, S. *J. Am. Chem. Soc.* **2001**, *123*, 11446. Muller, A.; Talbot, F.; Leutwyler, *J. Am. Chem. Soc.* **2002**, *124*, 14486.
(9) Tajima, Y.; Ishikawa, H.; Miyazawa, T.; Kira, M.; Mikami, N. *J. Am. Chem. Soc.* **1997**, *119*, 7400. Ebata, T.; Fujii, A.; Mikami, N. *Int. Rev. Phys. Chem.* **1998**, *17*, 331.
(10) Kleinermanns, K.; Gerhards, M.; Schmitt, M. *Ber. Bunsen-Ges. Phys. Chem.* **1997**, *101*, 1785.
(11) Lisy, J. M. *Int. Rev. Phys. Chem.* **1997**, *16*, 267.
(12) Castleman, A. W. *Adv. Gas Phase Ion Chem.* **1998**, *3*, 185.
(13) Keutsch, F. N.; Saykally, R. J. *Proc. Natl. Acad. Sci. U.S.A.* **2001**, *98*, 10533.
(14) Kim, K. S.; Tarakeshwar, P.; Lee, J. Y. *Chem. Rev.* **2000**, *100*, 4145.
(15) Gavezotti, A. *CrystEngComm* **2003**, *5*, 429. Gavezotti, A. *CrystEngComm* **2003**, *5*, 439.
(16) Gohlke, H.; Klebe, G. *Angew. Chem., Int. Ed.* **2002**, *41*, 2644.

10.1021/ja056454j CCC: $33.50

Intermolecular complexes of π-systems and ammonia (**Am**) are prototypical models of aromatic−amino interactions, which were first observed in structures of haemoglobin−ligand complexes.[17] Furthermore, these interactions are widely prevalent in a number of protein crystal structures.[18−20] The recent elucidation of the crystal structure of the ammonia channels in a membrane highlights the importance of interactions involving aromatic residues in the transport of ammonia across the membrane of a cell.[21] However, the structural influence and functional relevance of these interactions are still a matter of debate, because little is known about their exact nature.[14,22] Amines, in particular ammonia, are generally considered to be amphoteric; i.e., they can behave as donors or acceptors in terms of their hydrogen-bonding ability. However, the tendency of ammonia to act as a proton acceptor is deeply pronounced, reflecting its large proton affinity.[23]

An ammonia molecule can interact with an aromatic molecule either through the formation of a conventional hydrogen bond with an electron-rich substituent at the aromatic ring (σ-type of interaction) or by a hydrogen bond with the electron cloud of the π-system (π-type of interaction). Despite the fairly large number of theoretical and experimental investigations of intermolecular complexes containing ammonia, there are relatively few studies on systems exhibiting the π···H−N interactions.[24−38] This is because, the relatively small intermolecular interaction energies of these systems make it very difficult to characterize them experimentally.[24−34] Furthermore, as these interactions are dominated by dispersion energies, theoretical calculations are tenuous because electron correlation has to be explicitly taken into account at a rather high computational level.[35−38]

In a number of previous studies, we have extensively illustrated the modulation of the OH− vibrational frequencies of π−(water)$_n$ complexes as a result of changes in both the electron density of the π-system by substituents and by an incremental addition of water molecules.[39,40] Given the importance of ammonia containing π complexes, we consider it a fundamental issue to study in a similar way the modulation of their structures, energies, and vibrational spectra with ammonia as a result of changes in the details of the π-system. We employ the IR/R2PI vibrational spectroscopic method, which is based on IR-induced vibrational predissociation spectroscopy detected mass selectively by resonant two-photon ionization mass spectroscopy (R2PI), to experimentally investigate a number of π−ammonia complexes {benzene (**Bz**), fluorobenzene (**FBz**), *p*-difluorobenzene (**pDFBz**), chlorobenzene (**ClBz**, toluene (**Tol**)} in the region of the N−H stetches.

Among the π−**Am** complexes exhibiting a π-H-bonding interaction, the **Bz**−**Am** dimer is a frequently studied cluster system.[24−26] Its microwave spectrum indicates the presence of a π-H-bond between one of the hydrogens of ammonia and the benzene π-system.[24] In the experimentally derived structure, the C_3 symmetry axis of ammonia is tilted by about 58° relative to the benzene C_6 axis. While the experimental dissociation energy of the **Bz**−**Am** complex has been found to be 1.84 ± 0.12 kcal/mol,[25] there has been hitherto no investigation on the infrared (IR) vibrational spectra of this complex.

In addition to the experimental investigation of the vibrational spectra in the NH-stretch region, we have carried out high-level ab initio calculations of these complexes. A comparison of the calculated and experimental vibrational spectra allows the assignment of the structure of the complexes. Moreover, a detailed decomposition of the interaction energies was carried out using the symmetry adapted perturbation theory (SAPT) method,[41−43] to delineate the factors responsible for the stability of various conformers of π−ammonia and π−water complexes. For comparison, theoretical results on the interaction of ammonia with ethene, representing the prototype of an olefinic π-system, are included.

(17) Perutz, M. F.; Fermi, G.; Abraham, D. J.; Poyart, C.; Bursaux, E. *J. Am. Chem. Soc.* **1986**, *108*, 1064.
(18) Burley, S. K.; Petsko, G. A. *FEBS Lett.* **1986**, *203*, 139.
(19) Levitt, M.; Perutz, M. F. *J. Mol. Biol.* **1988**, *201*, 751.
(20) Steiner, T.; Koellner, G. *J. Mol. Biol.* **2001**, *305*, 535. Mao, L. S.; Wang, Y. L.; Liu, Y. M.; Hu, X. C. *J. Mol. Biol.* **2004**, *336*, 787.
(21) Khademi, S.; O'Connell, J.; Remis, J.; Robles-Colmenares, Y.; Miercke, L. J. W.; Stroud, R. M. *Science* **2004**, *305*, 1587.
(22) Meyer, E. A.; Castellano, R. K.; Diederich, F. *Angew. Chem., Int. Ed.* **2003**, *42*, 1210.
(23) Wu, R.; Vaupel, S.; Nachtigall, P.; Brutschy, B. *J. Phys. Chem. A* **2004**, *108*, 3338.
(24) Rodham, D. A.; Suzuki, S.; Suenram, R. D.; Lovas, F. J.; Dasgupta, S.; Goddard, W. A., III; Blake, G. A. *Nature* **1993**, *362*, 735.
(25) Mons, M.; Dimicoli, I.; Tardivel, B.; Piuzzi, F.; Brenner, V.; Millié, P. *Phys. Chem. Chem. Phys.* **2002**, *4*, 571.
(26) (a) Ritze, H.-H.; Lippert, H.; Stert, V.; Radloff, W.; Hertel, I. V. *J. Chem. Phys.* **2004**, *120*, 3619. (b) Weyers, K.; Freudenberg, Th.; Ritze, H.-H.; Radloff, W.; Stert, V. *Z. Phys. D* **1997**, *39*, 217. (c) Radloff, W.; Freudenberg, Th.; Stert, V.; Ritze, H.-H.; Noack, F.; Hertel, I. V. *Chem. Phys. Lett.* **1997**, *264*, 210. (d) Radloff, W.; Freudenberg, Th.; Stert, V.; Ritze, H.-H.; Weyers, K.; Noack, F. *Chem. Phys. Lett.* **1996**, *258*, 507. (e) Radloff, W.; Freudenberg, Th.; Ritze, H.-H.; Stert, V.; Weyers, K.; Noack, F. *Chem. Phys. Lett.* **1995**, *245*, 400.
(27) (a) Dedonder-Lardeux, C.; Dimicoli, I.; Jouvet, C.; Martrenchard-Barra, S.; Richard-Viard, M.; Solgadi, D.; Vervloet, M. *Chem. Phys. Lett.* **1995**, *240*, 97. (b) Grgoire, G.; Dedonder-Lardeux, C.; Jouvet, C.; Martrenchard, S.; Peremans, A.; Solgadi, D. *J. Phys. Chem. A.* **2000**, *104*, 9087. (c) Grgoire, G.; Dedonder-Lardeux, C.; Jouvet, C.; Martrenchard, S.; Solgadi, D. *J. Phys. Chem. A* **2001**, *105*, 5971.
(28) Li, S.; Bernstein, E. R. *J. Chem. Phys.* **1991**, *95*, 1577.
(29) Schiefke, A.; Deusen, C.; Jacoby, C.; Gerhards, M.; Schmitt, M.; Kleinermanns, K.; Hering, P. *J. Chem. Phys.* **1995**, *102*, 9197. Schmitt, M.; Jacoby, Ch.; Gerhards, M.; Unterberg, C.; Roth, W.; Kleinermanns, K. *J. Chem. Phys.* **2000**, *113*, 2995.
(30) Fedorov, A. V.; Cable, J. R.; Carney, J. R.; Zwier, T. S. *J. Phys. Chem. A* **2001**, *105*, 8162.
(31) Fernández, J. A.; Longarte, A.; Unamuno, I.; Castaoa, F. *J. Chem. Phys.* **2000**, *113*, 8541. Longarte, A.; Fernández, J. A.; Unamuno, I.; Castañoa, F. J. *J. Chem. Phys.* **2000**, *113*, 8549.
(32) Peschke, M.; Blades, A.; Kebarle, P. *J. Am. Chem. Soc.* **2002**, *124*, 11519.
(33) van Wijngaarden, J.; Jäger, W. *J. Am. Chem. Soc.* **2003**, *125*, 14631.
(34) Beu, T. A.; Buck, U. *J. Chem. Phys.* **2001**, *114*, 7848. Beu, T. A.; Buck, U. *J. Chem. Phys.* **2001**, *114*, 7853.
(35) Enkvist, C.; Zhang, Y.; Yang, W. *Int. J. Quantum Chem.* **2000**, *79*, 325.
(36) Tsuzuki, S.; Honda, K.; Uchimaru, T.; Mikami, M.; Tanabe, K. *J. Am. Chem. Soc.* **2000**, *122*, 11450.
(37) Tarakeshwar, P.; Choi, H. S.; Kim, K. S. *J. Am. Chem. Soc.* **2001**, *123*, 3323.
(38) Tarakeshwar, P.; Kim, K. S. *J. Mol. Str.* **2002**, *615*, 227.
(39) (a) Barth, H.-D.; Buchhold, K.; Djafari, S.; Reimann, B.; Lommatzsch, U.; Brutschy, B. *Chem. Phys.* **1998**, *239*, 49. (b) Riehn, C.; Reimann, B.; Buchhold, K.; Vaupel, S.; Barth, H.-D.; Brutschy, B.; Tarakeshwar, P.; Kim, K. S. *J. Chem. Phys.* **2001**, *115*, 10045. (c) Reimann, B.; Buchhold, K.; Barth, H.-D.; Brutschy, B.; Tarakeshwar, P.; Kim, K. S. *J. Chem. Phys.* **2002**, *117*, 8805.
(40) (a) Tarakeshwar, P.; Choi, H. S.; Lee, S. J.; Lee, J. Y.; Kim, K. S.; Ha, T.-K, Jang, J. H.; Lee, J. G.; Lee, H. *J. Chem. Phys.* **1999**, *111*, 5838. (b) Tarakeshwar, P.; Kim, K. S.; Brutschy, B. *J. Chem. Phys.* **1999**, *110*, 8501. (c) Tarakeshwar, P.; Kim, K. S.; Brutschy, B. *J. Chem. Phys.* **2000**, *112*, 1769. (d) Tarakeshwar, P.; Kim, K. S.; Brutschy, B. *J. Chem. Phys.* **2001**, *114*, 1295. (e) Tarakeshwar, P.; Kim, K. S.; Djafari, S.; Buchhold, K.; Reimann, B.; Barth, H.-D.; Brutschy, B. *J. Chem. Phys.* **2001**, *114*, 4016.
(41) Jeziorski, B.; Szalewicz, K. In *Encyclopedia of Computational Chemistry*; Schleyer, P. v. R., Allinger, N. L., Clark, T., Gasteiger, J., Kollman, P. A., Schaefer, H. F., III, Schreiner, P. R., Eds.; Wiley: Chichester, U.K., 1998.
(42) Jeziorski, B.; Moszynski, R.; Szalewicz, K. *Chem. Rev.* **1994**, *94*, 1887. Szalewicz, K.; Jeziorski, B. In *Molecular Interactions − From van der Waals to Strongly Bound Complexes*; Scheiner, S., Ed.; Wiley: New York, 1997; p 3.
(43) Jeziorski, B.; Moszynski, R.; Ratkiewicz, A.; Rybak, S.; Szalewicz, K.; Williams, H. L. In *Methods and Techniques in Computational Chemistry: METECC-94*; Clementi, E., Ed.; Medium Sized Systems, Vol. B; STEF: Cagliari, 1993; pp 79−129.

Methodology

Experimental. Details of the experimental setup for the R2PI- and IR/R2PI-spectroscopy have already been published elsewhere.[44,45] Briefly, mixed clusters containing the aromatic chromophore and ammonia in various mixing ratios are produced in a 10-Hz-pulsed seeded supersonic expansion with the sample gases diluted at typical concentrations of 0.01−1% in helium (p_0 = 2 bar). The 1:1 clusters are ionized via one-color R2PI (1C-R2PI) utilizing the frequency-doubled output of an excimer pumped, pulsed dye laser. The photo ions are mass analyzed in a reflectron time-of-flight mass spectrometer. The amplified (10×) ion signal is digitized in a transient recorder (LeCroy TR8828C), programmed in multiboxcar mode. The mass spectra are typically averaged over 100−200 laser pulses.

The R2PI spectrum of a specific ion represents the wavelength dependence of its ion yield curve. Due to the resonant step in the two-photon process, it reflects the UV absorption spectrum of the neutral precursor. A cluster of particular size and structure can be investigated by tuning the ionization laser to specific transitions in its R2PI spectrum. The vibrational spectrum of the neutral precursor may be recorded by utilizing IR/R2PI depletion spectroscopy.[44−46] In this technique an IR-laser pump pulse precedes the UV laser by about 70 μs with both lasers overlapping with the cluster beam. In case a cluster absorbs photons with energies of one or several quanta of a high-frequency vibrational mode, it predissociates very fast by IVR resulting in a depopulation and R2PI-ion signal depletion. An ion-dip spectrum is recorded by scanning the wavelength of the IR laser with the wavelength of the probe laser being fixed to the transition of a selected cluster. It represents part of the vibrational spectrum of the neutral precursor cluster in the electronic ground state and is termed in the following an IR/R2PI vibrational spectrum.[2]

In spite of the mass selectivity R2PI spectra often contain spectral features from larger fragmenting clusters or from different structural isomers. To attain both isomer and size selectivity, IR/UV hole burning spectroscopy may be applied which allows the assigments of the bands in an R2PI spectrum originating from the same precursor. For this the wavelength of the IR laser is fixed to a prominent and unique vibrational band of the species under study while the wavelength of the UV laser is scanned. The intensity of the transitions in the R2PI spectrum belonging to the same precursor are decreased similarly, while those originating from other isomers/sizes will be left unchanged. The difference spectrum with the IR laser off and on contains then bands of the absorbing species.

IR laser light is generated by a home-built, injection-seeded OPO utilizing $LiNbO_3$ crystals and an Nd:YAG pump laser. Typical energies are about 5 mJ/pulse. The wavelength may be tuned in the range 2.5−4.0 μm with a bandwidth of 0.2 cm^{-1}. To avoid saturation effects the IR energy is usually reduced to ∼1.5 mJ/pulse. The mildly focused IR beam was directed coaxially into the supersonic beam, while the beam of the ionizing laser crosses both beams at a right angle.

Benzene (99.7%) and toluene (99.7%) were purchased from Riedel-de Haën, fluorobenzene (99.5%) was purchased from Fluka, chlorobenzene (99%+) and *p*-chlorofluorobenzene (98%) were purchased from Acros, *p*-Difluorobenzene was purchased (99%+) from Janssen, and 1% ammonia in helium was purchased from Messer. All substances are used without further purification.

Computational Details. Both, the supermolecular (SM) variational and perturbational (SAPT) methods were employed to investigate the π-**Am** complexes described in this study.[41−43,47] Even though the former method is conceptually and computationally simple, it does not provide a (clear) detailed picture of the interaction forces responsible for the interaction. On the other hand, the latter method provides a physical picture of the interactions prevailing between the molecules. This is because of the fact that the SM-interaction energy is evaluated as the difference of the energy of the complex and the energy of the separated and isolated monomers, and the SAPT-energy, as a sum of the individual *electrostatic, exchange, dispersion, and induction* energies. The calculations are briefly described to aid the discussion of the computational results.

We initially carried out the geometry optimizations and evaluated the vibrational frequencies using both the 6-31+G* and aug-cc-pVDZ basis sets, at the second-order Møller−Plesset (MP2) level of theory.[48−51] Given the importance of dispersion interactions in the description of these complexes, we also carried out calculations using the larger aug-cc-pCVDZ, aug-cc-pVTZ, and aug-cc-pVQZ basis sets.[52] While both the aug-cc-pVTZ and aug-cc-pVQZ basis set calculations were carried out using the resolution of identity second-order Møller−Plesset (RIMP2) level of theory, the latter calculations could be carried out for the ethene and benzene complexes.[53] The effects of the inclusion of higher levels of correlation on the vibrational frequencies were examined by carrying out CCSD(T) {coupled-cluster with single, double, and perturbative triple substitutions} calculations on the smaller ethene−ammonia complex.[54] All the electrons were explicitly correlated in the MP2 and CCSD(T) calculations. For the sake of brevity, the results obtained at the MP2/aug-cc-pVDZ or higher calculation levels are discussed. The other results are presented in a supplementary table.

The zero-point vibrational energy (ZPVE) corrections were computed from frequencies evaluated at the MP2/6-31+G* and MP2/aug-cc-pVDZ levels of theory. Basis set superposition error (BSSE) corrections were carried out for all complexes using the counterpoise (CP) method of Boys and Bernardi.[55] Since BSSE also affects the calculated geometries and vibrational frequencies, we have also carried out BSSE-corrected geometry optimizations.[38,56] The BSSE-corrected vibrational frequencies and the ZPVE corrections were then obtained on the BSSE-corrected geometries. The SM calculations were carried out using the GAUSSIAN, TURBOMOLE, and ACES2 suite of programs.[57−59]

In this study, the SAPT calculations were carried out using the MP2/aug-cc-pVDZ optimized geometries (obtained from SM calculations) of all the complexes. The SAPT interaction energy (E_{int}) can be approximated as a sum of electrostatic (E_{es}), induction (E_{ind}), dispersion (E_{disp}), and exchange (E_{exch}) terms. Since BSSE effects are explicitly included when evaluating the SAPT interaction energies, a comparison of the BSSE-corrected supermolecular interaction energy (ΔE_e^B) and the SAPT interaction energy (E_{int}) is appropriate. The SAPT interaction energy can also be represented as the sum of $E_{int}^{(HF)}$ and $E_{int}^{(corr)}$, where $E_{int}^{(HF)}$ is the sum of all the energy components evaluated at the Hartree−Fock (HF) level and $E_{int}^{(corr)}$ is the sum of all the energy components evaluated at the correlated level. Given the size of the systems investigated and the level of theory (aug-cc-pVDZ) employed in this study to evaluate the various energy components, it was not

(44) Riehn, C.; Lahmann, C.; Wassermann, B.; Brutschy, B. *Chem. Phys. Lett.* **1992**, *197*, 443.
(45) Riehn, C.; Lahmann, C.; Wassermann, B.; Brutschy, B. *Ber. Bunsen-Ges. Phys. Chem.* **1992**, *96*, 1161.
(46) (a)Page, R. H.; Shen, Y. R.; Lee, Y. T. *J. Chem. Phys.* **1989**, *88*, 4621. (b) Tanabe, S.; Ebata, T.; Fuji, M.; Mikami, N. *J. Phys. Lett.* **1993**, *215*, 347. (c) Pribble, R. N.; Zwier, T. *Science* **1994**, *265*, 75.
(47) Chalasinski, G.; Szczesniak, M. M. *Chem. Rev.* **1994**, *94*, 1723. Chalasinski, G.; Szczesniak, M. M. *Chem. Rev.* **2000**, *100*, 4227.
(48) Møller, C.; Plesset, M. S. *Phys. Rev.* **1934**, *46*, 618.
(49) Hehre, W. J.; Ditchfield, R.; Pople, J. A. *J. Chem. Phys.* **1972**, *56*, 2257.
(50) Dunning, T. H. *J. Chem. Phys.* **1989**, *90*, 1007.
(51) Kendall, R. A.; Dunning, T. H.; Harrison, R. J. *J. Chem. Phys.* **1992**, *96*, 6796.
(52) Woon, D. E.; Dunning, T. H. *J. Chem. Phys.* **1993**, *103*, 4572.
(53) Weigend, F.; Hser, M. *Theor. Chim. Acc.* **1997**, *97*, 331.
(54) Raghavachari, K.; Trucks, G. W.; Pople, J. A.; Head-Gordon, M. *Chem. Phys. Lett.* **1989**, *157*, 479. Bartlett, R. J. *J. Phys. Chem.* **1989**, *93*, 1697.
(55) Boys, S. F.; Bernardi, F. *Mol. Phys.* **1970**, *19*, 553.
(56) Simon, S.; Duran, M.; Dannenberg, J. J. *J. Chem. Phys.* **1996**, *105*, 11024. Salvador, P.; Paizs, B.; Duran, M.; Suhai, S. *J. Comput. Chem.* **2000**, *22*, 765.
(57) Frisch, M. J. et al. *Gaussian 98*, revision A.11; Gaussian, Inc.: Pittsburgh, PA, 2001.
(58) Ahlrichs, R.; Bär, M.; Häser, M.; Horn, H.; Kölmel, C. *Chem. Phys. Lett.* **1989**, *162*, 165.
(59) Stanton, J. F. et al. ACES II, Quantum Theory Project, University of Florida: Gainesville, FL.

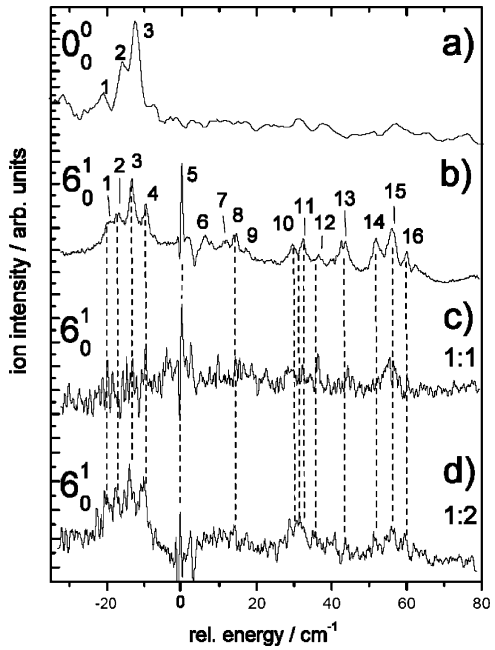

Figure 1. R2PI spectra measured for $Bz^+ \cdot NH_3$ (a) near the vibrationless $S_1 \leftarrow S_0$ electronic transition (0_0^0) transition of Bz and (b) near its 6_0^1 transition. Difference spectra of trace b with the IR-depletion laser tuned (c) to 3441 cm^{-1} and (d) to 3404 cm^{-1}.

feasible to evaluate the computationally demanding higher order components ($n \leq 3$). Hence, one should expect a slight deviation of the total interaction energies evaluated using SAPT and SM calculations. This however does not influence the conclusions based on the magnitude of the individual interaction energy components, as was shown in a number of recent papers. A detailed description of SAPT and some of its applications can be found in some recent references.[37,38,41−43,60−64]

Results and Discusssion

Experimental. Benzene/Ammonia Cluster. The R2PI spectrum of the **Bz−Am** cluster, recorded for the $Bz^+ \cdot NH_3$ signal in the vicinity of the vibrationless $S_1 \leftarrow S_0$ electronic transition (0_0^0) of benzene (38 086 cm^{-1}), is depicted in Figure 1a. Three weakly red-shifted bands 1−3 appear for the cluster. This is in stark contrast to the isolated monomer for which the transition is symmetry forbidden. As will be justified in the following, these bands are assigned to the 1:2 complex fragmenting into the 1:1 ion chanel. The first intense transition of the monomer is the 6_0^1 at 38 606 cm^{-1}. The R2PI spectrum of the 1:1 cluster recorded in this region is depicted in Figure 1b. The energy of the bands is given relative to the 6_0^1 transition of the monomer. As already reported in previous studies,[15,24,26b] a richly structured vibrational band pattern shows up.

The band positions are listed in Table 1 together with our assignment and that from literature. The assignment from an R2PI spectrum alone may be prone to error, since some bands may be from larger fragmenting clusters or from different confomers of the same size. Therefore IR/R2PI vibrational spectra and IR/UV hole burning scans should clarify ambiguities. For the latter we recorded the R2PI spectrum with the IR laser tuned to 3441 cm^{-1}, corresponding to a transition in the vibrational spectrum assigned to the 1:1 complex (Figure 2a) as will be discussed below.

Comparing the spectra with the IR laser off and on all bands which originate from the same precursor should be similarly

Table 1. Position of the Bands in the R2PI Spectrum of $\mathbf{Bz}^+ \cdot NH_3$ in Figure 1 and Their Assignment

	rel. position in cm^{-1} of (band)	assignment(s): [1]this work, [2]Weyers et al.,[26b] [3]Rodham[24]
Bz 0_0^0	−21 (1), −16 (2),	$1:2^1$, *1:1(I)*^{2}
	−13 (3)	$1:2^1$
Bz 6_0^1	−19 (1), −17 (2)	$1:2^1$, *1:1 (I)*^{2}
	−13 (3), −10 (4)	$1:2^1$
	0 (5)	$1:1^1$, *1:1 (II)*
	+6 (6), +12 (7)	
	+15 (8)	$1:2^1$
	+17 (9)	
	+30 (10), 32 (11), +36 (12)	$1:2^1$, *1:1 (Ia)*^{2}
	+43, +44 (13)	$1:1,^1$ *1:1 (IIa)*^{2}
	+52 (14)	$1:2,^1$ *1:1*^{3}, *1:1 (Ib)*^{2}
	+56 (15)	$1:1,^1$ $1:2,^2$ *1:1*^{3}, *1:1 (Ib)*^{2}
	+60 (16)	$1:2,^1$ *1:1 (Ib)*^{3}
Tol	−55 (1), −5 (3)	$1:1,^1$ Tπ_1
	−50 (2), −24 (5), +22(4)	$1:1,^1$ Tπ_2
	+6 (6)	

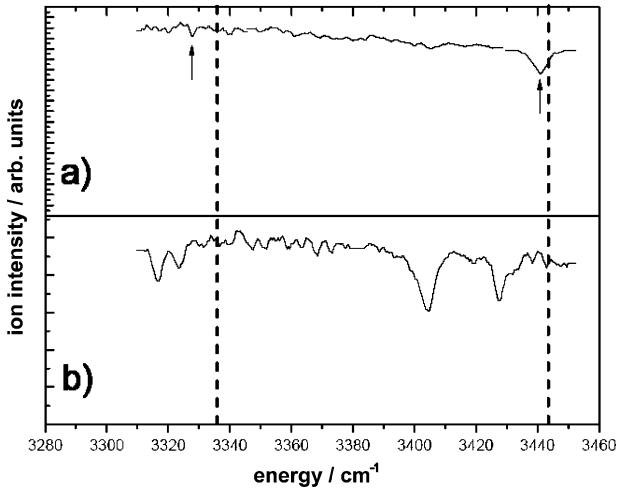

Figure 2. IR/R2PI spectrum measured for $Bz^+ \cdot NH_3$ with the UV laser tuned to (a) the prominent band 5 in Figure 1b, assigned to the 1:1 complex and (b) the prominent band 3 in Figure 1b, assigned to the 1:2 complex.

depleted. The differential depletion spectrum, which is thus assigned to the 1:1 complex, is depicted in Figure 1c. In Figure 1b, the spectrum contains on a rather noisy baseline, due to a weak depletion of a relatively low signal, band 5 as the dominant one of all the bands and bands 12 and 13 and a broad feature near band 15. With the IR laser tuned to 3404 cm^{-1}, corresponding to a band assigned in the following to the vibrational spectrum of the 1:2 complex (Figure 2b), a different differential spectrum is observed (Figure 1d). Those features which are missing in Figure 1c as compared to Figure 1b are now the strongest. The group of bands 1−4 dominates the spectrum. However broader noisy bands appear where bands 10, 11, and 14−16 appear in Figure 1b. Hence we assign these bands to the 1:2 cluster, which is detected in the $Bz^+ \cdot NH_3$ ion channel due to fragmentation. From high-resolution R2PI spectra Rodham et al. assigned bands 14 and 15 located at about +57 cm^{-1} as the only bands originating from the 1:1 cluster. All other resonances were attributed by these authors to fragmenting clusters with more than one ammonia molecule.[24]

Weyers and co-workers, on the other hand, assigned bands 14 and 15 to intermolecular vibrations of an isomer exhibiting its vibrational origin at −20 cm^{-1}. They assigned a second isomer of the 1:1 cluster with an origin starting with band 5,[26b] which we assign to the 1:1 complex. Neither the R2PI hole

Table 2. Shifts of the NH Stretching Vibrations of the Different 1:1 Complexes Taken from the IR/R2PI Spectra Measured at Cluster Specific UV Transitions (Given in Column 1 as Values Relative to the Transition in the Monomer Indicated in parentheses)[a]

chromophore R2PI transition of the 1:1 complex relative to that in the monomer	$\Delta\nu_1(1)$	$\Delta\nu_3(1)$	$\Delta\nu_3(2)$	$\delta\Delta\nu 3$
Bz ($\nu_{06} = 38\,603$) $6_0^1 \pm 0$	−8.3		−2.6	0
Tol π_1 ($\nu_{00} = 37\,477$) $0_0^0 - 55$	−9.8	−20.5	+3.7	24.2
Tol π_2 ($\nu_{00} = 37\,477$) $0_0^0 - 50$	−9.8		−8.9	0
FBz ($\nu_{00} = 37\,816$) $0_0^0 + 58.7$	−3.1		−3.6	0
ClBz ($\nu_{00} = 37\,063$) $0_0^0 + 78$	−6.6	−15.6	−4.5	11.1
pDFBz ($\nu_{00} = 36\,838$) $0_0^0 + 97$	−1.9	−11.1	−4.1	7.0
pClFBz ($\nu_{00} = 36\,276$) $0_0^0 + 100$	−6.1		−3.6	0

[a] The experimental values of the stretching vibrations of ammonia relative to the reference values for the two energy regions. The latter are the symmetric $\nu_1 = 3336.1$ cm^{-1} and the asymmetric $\nu_3 = 3443.6$ cm^{-1} of ammonia.[65] $\delta\Delta\nu_3$ is the splitting of the asymmetric vibration in the clusters. All units are cm^{-1}.

burning spectra nor the IR/R2PI vibrational spectra gave evidence for the occurrence of a second 1:1 isomer as assigned by Mons et al.[25] and Weyers.[26b] However, the second isomer of the 1:1, assigned by Rodham et al. and Weyers, is clearly a 1:2 complex as is evident from the vibrational spectra discussed in the following.

Figure 2a represents the IR/R2PI spectrum with the UV laser tuned to the prominent band 5 in Figure 1b, assigned to the 1:1 complex. Two weak but reproducible absorption bands can be observed at 3327.8 and 3441.0 cm^{-1}. For comparison the isolated ammonia[65,66] has a symmetric stretching mode ν_1 at 3336.1 cm^{-1} and an asymmetric stretching mode ν_3 at 3443.6 cm^{-1}, both of which are indicated in Figure 2 by the dashed lines. Relative to these bands the modes of the bonded ammonia are red-shifted by 8.3 and 2.6 cm^{-1}, respectively. Due to the existence of only two absorption bands at beam conditions where larger clusters exist only in spurious amounts, this spectrum is assigned to the **Bz**−**Am** complex.

The IR/R2PI spectrum measured for the $Bz^+ \cdot NH_3$ ion signal with the UV laser tuned to the dominant band 3 in Figure 1a or 1b is depicted in Figure 2b. It contains at least four prominent vibrational bands. Thus it cannot originate from any isomer of the 1:1 but must be due to a larger complex. Since it appears already at very low relative concentrations of ammonia in the beam, when $1^+{:}n > 3$ clusters do not appear in the mass spectrum, we assign this vibrational spectrum to the 1:2 complex. The band positions are listed in Table 2 together with the spectroscopic shifts. The fact that bands 1 to 3 appear both in the vicinity of the 6_0^1 and the 0_0^0 transition of the monomer

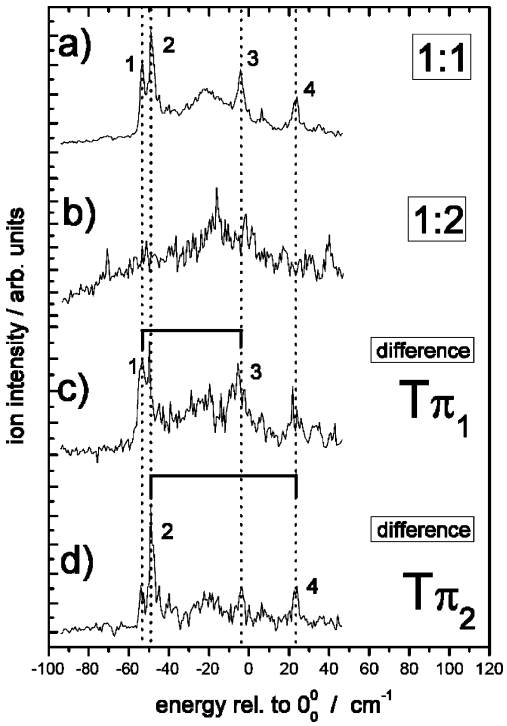

Figure 3. R2PI spectra measured (a) near the vibrationless $S_1 \leftarrow S_0$ electronic transition (0_0^0) transition for $To^+ \cdot NH_3$ and (b) for $To^+ \cdot (NH_3)_2$. Difference spectra of trace (a) with the IR-depletion laser tuned in (c) to 3441 cm^{-1} and in (d) to 3404 cm^{-1}. The spectra in (c) and (d) are assigned to different isomers **T**π_1 and **T**π_2, respectively, of the 1:1 complex.

with nearly the same shift indicates that the bands in Figure 1a are due to fragmentation. For larger complexes the IR/R2PI spectra, not shown here, consist of mainly two bands at 3323 and 3427 cm^{-1} which are more strongly red-shifted and broader than those in Figure 2 and show only a weak size dependence.

Toluene/Ammonia Cluster. The R2PI spectrum of the system **Tol**−**Am** has been reported previously in detail.[67,68] The spectrum of the $1{:}1^+$ complex is monitored by the yield of the $(NH_3)H^+$ ion. The latter is the product of a dissociative proton-transfer reaction taking place in the $(1{:}1)^+$ complex. The R2PI spectrum is dominated by four absorption bands 1−4. Li and Bernstein[67] assigned these bands to clusters with three and four ammonia molecules fragmenting after R2PI into the 1:1 ion channel. IR/UV hole burning spectra, depicted in Figure 3c and d, were recorded with the IR laser tuned to either 3336.7 cm^{-1} or 3443.8 cm^{-1}. At these wavelengths either the bands 1 and 3 or the bands 2 and 4 are strongly depleted.

The IR/R2PI spectra measured with the UV laser tuned to band 1 and band 2, respectively, are depicted in Figure 4a and 4b, respectively. They clearly differ from each other and thus may be assigned to different species. Since only two or three bands are observed, the assignment of two 1:1 isomers seems to be compelling. If the vibrational spectra would be due to larger complexes additional vibrations should appear and the R2PI bands should have a different dependence from the expansion conditions, which is not observed.

(60) Bukowski, R.; Szalewicz, K.; Chabalowski, C. *J. Phys. Chem. A* **1999**, *103*, 7322.
(61) Milet, A.; Moszynski, R.; Wormer, P. E. S.; van der Avoird, A. *J. Phys. Chem. A* **1999**, *103*, 6811.
(62) Visentin, T.; Kochanski, E.; Moszynski, R.; Dedieu, A. *J. Phys. Chem. A* **2001**, *105*, 2023. Visentin, T.; Kochanski, E.; Moszynski, R.; Dedieu, A. *J. Phys. Chem. A* **2001**, *105*, 2031.
(63) Tarakeshwar, P.; Kim, K. S.; Kraka, E.; Cremer, D. *J. Chem. Phys.* **2001**, *115*, 6018.
(64) Kim, D.; Hu, S.; Tarakeshwar, P.; Kim, K. S.; Lisy, J. M. *J. Phys. Chem. A* **2003**, *107*, 1128. Kim, D.; Tarakeshwar, P.; Kim, K. S. *J. Phys. Chem. A* **2004**, *108*, 1250.
(65) (a) Spirko, V. Kraemer, W. P. D. *J. Mol. Spectrosc.* **1989**, *133*, 331. (b) Angstl, R.; Finsterholzl, H.; Frunder, H.; Illig, D.; Papouek, D.; Pracna, P.; Rao, K. N.; Schrotter, H. W.; Urban, S. *J. Mol. Spectrosc.* **1983**, *101*, 1.
(66) Coy, S. L.; Lehmann, K. K. *Spectrochim. Acta A* **1989**, *45*, 47.
(67) (a) Brutschy, B.; Janes, C.; Eggert, J. *Ber. Bunsen-Ges. Phys. Chem.* **1988**, *92*, 435. (b) Eggert, J. Dissertation, Berlin, 1990. (c) Li, S.; Bernstein, E. R. *J. Chem. Phys.* **1992**, *97*, 804.
(68) (a) Thölmann, D.; Grützmacher, H. *Chem. Phys. Lett.* **1989**, *163* (2, 3), 225. (b) Thölmann, D.; Grützmacher, H. *Chem. Phys. Lett.* **1991**, *113* (9), 3281.

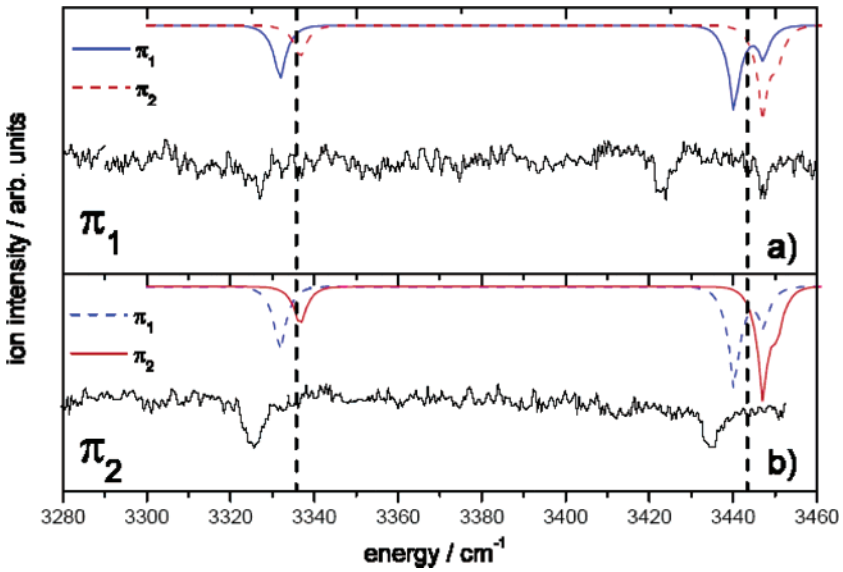

Figure 4. IR/R2PI spectra measured with the UV tuned (a) to band 1 and (b) to band 2 in Figure 3a. The solid and dashed lines are the results from the calculated π_1- and π_2-isomer. The best fit is represented by a solid line.

Hence we assign each band pair to a different isomer of the **Tol−Am** complex, termed in the following isomer **Tπ_1** and **Tπ_2**. In the difference hole burning spectra in Figure 3c, we assign band 1 as the origin band of isomer **Tπ_1** and band 3 to an intramolecular vibration of 50 cm $^{-1}$. Band 2 in Figure 3d is assigned as the origin of the second isomer **Tπ_2** exhibiting an intramolecular vibration of 72 cm^{-1} (band 4). This assignment will be supported by the results from the calculations. Surprisingly in the vibrational spectrum of **Tπ_1** (Figure 4a) three bands appear in the NH stretch region: one near the symmetric mode ν_1 of isolated ammonia and two in the region of the degenerate asymmetric vibration ν_3.

In the cluster the bands at 3423.1 and 3447.3 cm^{-1} are shifted by −20.5 and +3.7 cm^{-1} relative to the ν_3 mode of the isolated monomer. The splitting is indicative of a substantial perturbation of the symmetry of the ammonia molecule when interacting with toluene. In stark contrast to this, the vibrational spectrum of the **Tπ_2** isomer (Figure 4b) shows only a single band in this spectral region at 3434.7 cm^{-1}, corresponding to a shift of −8.9 cm^{-1}. The vibrational bands assigned to the symmetrical vibrations are located at nearly the same energy for both isomers, i.e., at 3326.3 cm^{-1} (−10.0 cm^{-1}) for the **Tπ_1** and at 3327.3 cm^{-1} (−9.0 cm^{-1}) for the **Tπ_2**. These red shifted bands are tentatively assigned to a weak H-bond formed between the ammonia and the aromatic system of toluene. The weak intensity of the bands also supports the assumption that stronger H-bonds do not exist as expected for larger ammonia subcomplexes. Therefore for both isomers a similar docking H-bond may be assumed.

Halobenzene/Ammonia Clusters. The R2PI spectra have been published elsewhere.[2] The IR/R2PI spectra recorded with the UV laser tuned to the transitions assigned to the 1:1 clusters in the R2PI spectra of **FBz·Am**, **ClBz·Am**, and **pDFBz·Am** are shown in Figure 5a−c. The positions of the vibrational absorption bands and of the vibronic origins excited in the R2PI spectra are tabulated in Table 2. For comparison we also include the positions of the bands for *p*-chlorofluorobenzene−**Am**, not shown in Figure 5. The IR/R2PI vibrational spectrum of the **FBz·Am** cluster depicted in Figure 5a was recorded for the 1:1$^+$

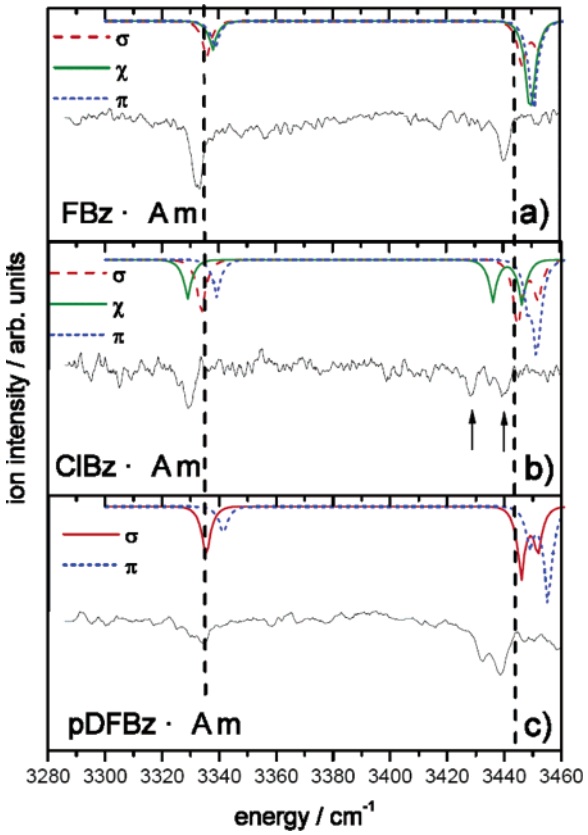

Figure 5. IR/R2PI spectra measured (a) for **FBz·**NH_3, (b) **ClBz·**NH_3, and (c) **pDFBz·**NH_3. The calculated spectra for the respective σ, χ, π isomers are given for comparison. The best fit is represented by a solid line.

ion channel. It shows two sharp and intense bands. The spectrum of the **ClBz·Am** cluster was recorded in the ion channel of the anilinium$^+$ ion, which appears as a product of a fast and nearly quantitative nucleophilic substitution reaction between chlorobenzene$^+$ and ammonia.[9,67,68] Similar to the spectrum of the **Tπ_1** isomer of **Tol−Am**, the asymmetric vibration is split up by 11.1 cm^{-1} (marked with arrows). The spectrum of the **pDFBz·Am** complex resembles only superficially that of the **ClBzAm** complex: both clusters exhibit a ν_3 splitting. However,

Table 3. Calculated Interaction Energies, Selected Geometrical Characteristics, and Vibrational Frequencies of the Ethene−**Am** Complex at Various Levels of Theory[a]

	aug-cc-pVDZ			aug-cc-pCVDZ			aug-cc-pVTZ		aug-cc-pVQZ
	MP2	MP2(BSSE)[b]	CCSD(T)	MP2	MP2(BSSE)[b]	CCSD(T)	MP2	RIMP2	RIMP2
$-\Delta E^{N}_{e}$	2.22	2.12	2.12	2.21	2.13	2.09	2.19	2.18	1.86
$-\Delta E^{B}_{e}$	1.28	1.40	1.13	1.33	1.40	1.30	1.43	1.76	1.63
$-\Delta E_{e}$	1.75	1.76	1.62	1.77	1.77	1.69	1.81	1.97	1.75
$-\Delta E_{0}$	0.90	1.00	0.75	0.86	1.03	0.96	1.11	1.12[c]	
$R_{\pi-H(NH_3)}$	2.616	2.828	2.609	2.671	2.822	2.767	2.606	2.617	2.674
$R_{\pi-Hnb(NH_3)}$	4.104	4.242	4.093	4.057	4.203	4.220	4.085	4.102	4.103
$R_{\pi-N(NH_3)}$	3.530	3.609	3.522	3.469	3.615	3.542	3.512	3.544	3.483
$-\Delta\nu_3$	4.5(5)	4.0(5)	0.0(17)	5.9(5)	2.1(5)	−0.4(7)	5.4(8)		
$-\Delta\nu_3$	8.4(32)	8.9(16)	7.2(1)	9.2(20)	6.9(16)	4.1(1)	14.5(52)		
$-\Delta\nu_1$	7.2(14)	6.6(9)	4.1(15)	7.7(12)	4.5(9)	2.9(11)	8.5(15)		

[a] All energies are in kcal/mol, distances are in Å, frequency shifts are in cm^{-1}, and IR intensities are in KM/mol. ΔE^{N}_{e} and ΔE^{B}_{e} represent the supermolecular binding energy without and with basis set superposition error (BSSE) correction. E_e represents the average of ΔE^{N}_{e} and ΔE^{B}_{e}. ΔE_0 represents the zero-point vibrational energy (ZPVE) corrected ΔE_e. $R_{\pi-H(NH_3)}$, $R_{\pi-Hnb(NH_3)}$, and $R_{\pi-N(NH_3)}$ are the distances from the center-of-mass of ethene to the ammonia hydrogen pointing to the π-system, ammonia hydrogen pointing away from the π-system, and ammonia nitrogen. $\Delta\nu_3$ and $\Delta\nu_1$ are the vibrational frequency shifts with respect to the calculated values of ammonia monomer. The corresponding IR intensities are enclosed in parantheses beside them. [b] BSSE corrections were explicitly taken into account during geometry optimizations and vibrational frequency evaluations. [c] ZPVE corrections were made using the frequencies evaluated at the MP2/aug-cc-pVDZ level.

it should be noted that the splitting for ClBz is nearly 50% larger than that of pDFBz. Surprisingly the spectrum of the **FBz·Am** complex shows only one ν_3 mode. We also note that the observed $\Delta\nu_1$ values for **pDFBz·Am**, **FBz·Am**, and **ClBz·Am** complexes have a linear correlation to the polarizabilities of the corresponding system. This finding supports an argument that the interaction of **Am** with these π-systems is mediated through the π-system (π-H bond). This is in contrast to the spectra of **FBz** and **DFBz** with water, where identical bands and spectra appear due to the local in-plane H-bond between water and one F substituent.[39a,39b,69]

Computational. Several studies have shown that extremely high-level ab initio calculations are required to reproduce the experimental geometries and vibrational frequencies of ammonia.[65,66,70−76] Thus, anharmonic frequencies {3337.4 (ν_1) and 3435.1 (ν_3) cm^{-1}} evaluated at the CCSD(T)/cc-pVQZ level are close to the experimental frequencies of 3336.1 (ν_1) and 3443.6 (ν_3) cm^{-1}.[65] In the context of this study, it is interesting to note that the calculated MP2/aug-cc-pVDZ vibrational frequencies of 3483.7 (ν_1) and 3639.5 (ν_3) cm^{-1} are in close agreement with the experimentally determined harmonic frequencies of (3485, 3504 cm^{-1}) (ν_1) and (3624, 3592 cm^{-1}) (ν_3).[66,73,74] In the absence of high-level theoretical investigations detailing the modulation of the NH stretching shifts of ammonia upon its interaction with various systems, we have evaluated the interaction energies and the corresponding vibrational frequencies of a relatively small system (ethene−**Am**) at several levels of theory.

Table 3 illustrates that the magnitude of the total interaction energies of the ethene−**Am** complex evaluated at the MP2 level are nearly independent of the size of the basis sets. Thus, geometry optimizations at the RIMP2/aug-cc-pVQZ level yield BSSE corrected interaction energies which are very similar to those evaluated at the MP2/aug-cc-pVDZ level. Even though one carries out the extremely arduous and time-consuming BSSE corrected geometry optimizations, the BSSE corrected interaction energies do not differ substantially. When ZPVE corrections are carried out, small differences can be noted in the interaction energies obtained on the BSSE corrected and uncorrected geometries. Despite the similarity of the interaction energies, one can notice substantial differences in the geometries and the vibrational frequency shifts at various levels of theory.

It can also be seen from Table 3 that complexation with ethene leads to a splitting in the doubly degenerate ν_3 NH stretching frequency of ammonia. While the absolute values of the frequencies are extremely dependent on the basis set and theoretical method, the calculated vibrational shift with respect to the isolated ammonia monomer is generally more useful for comparison with the experiment. The calculated harmonic vibrational frequencies of the ethene−**Am** complex at the MP2/aug-cc-pVDZ level are 3476.5 (ν_1) and (3631.1, 3639.5) (ν_3) cm^{-1}, respectively. The inclusion of BSSE in the geometry optimizations and vibrational frequency evaluations leads to very small changes in the values of ν_1 (3477.1 cm^{-1}) and ν_3 (3630.6, 3635.6 cm^{-1}).

A calculation of the anharmonic vibrational frequencies on the MP2/aug-cc-pVDZ BSSE corrected geometries of the ethene−**Am** complex indicates that the two split ν_3 N−H stretching modes nearly coalesce (3456.5, 3456.8 cm^{-1}). We would however like to emphasize that this observation is isolated and no inferences can be made on the spectra of the larger π−**Am** complexes. The corresponding anharmonic value of ν_1 is 3322.5 cm^{-1}. It is interesting to note that a scaling of the harmonic ν_1 and ν_3, by factors of 0.95 and 0.96, respectively, yield the corresponding anharmonic values. Similar observations were made in a recent investigation on comparison of harmonic frequencies to the corresponding experimental vibrational frequencies.[77]

(69) (a) Djafari, S.; Lembach, G.; Barth, H.-D.; Brutschy, B. *Z. Phys. Chem.* **1996**, 195, 253. (b) Djafari, S.; Lembach, G.; Barth, H.-D.; Brutschy, B. *J. Chem. Phys.* **1997**, *107*, 10573. (c) Buchhold, K.; Reimann, B.; Djafari, S.; Barth, H.-D.; Brutschy, B.; Tarakeswar, P.; Kim, K. S. *J. Chem. Phys.* **2000**, *112*, 1844. (d) Riehn, C.; Buchhold, K.; Reimann, B.; Djafari, S.; Barth, H.-D.; Brutschy, B.; Tarakeshwar, P.; Kim, K. S. *J. Chem. Phys.* **2000**, *112*, 1170.
(70) Duncan, J. C.; Mills, I. M. *Spectrochim. Acta A* **1964**, *20*, 523.
(71) Morino, Y.; Kuchitsu, K.; Yamamoto, S. *Spectrochim. Acta A* **1968**, *24*, 335.
(72) Hoy, A. R.; Mills, I. M.; Strey, G. *Mol. Phys.* **1972**, *24*, 1265.
(73) Martin, J. M. L.; Lee, T. J.; Taylor, P. R. *J. Chem. Phys.* **1992**, *97*, 8361.
(74) Bartlett, R.; Del Bene, J. E.; Perera, S. A.; Mattie, R. P. *THEOCHEM* **1997**, *400*, 157.
(75) Thomas, J. R.; DeLeeuw, B. J.; Vacek, G.; Crawford, T. D.; Yamaguchi, Y.; Schaefer, H. F., III. *J. Chem. Phys.* **1993**, *99*, 403.
(76) Pesonen, J.; Miani, A.; Halonen, L. *J. Chem. Phys.* **2001**, *115*, 1243.

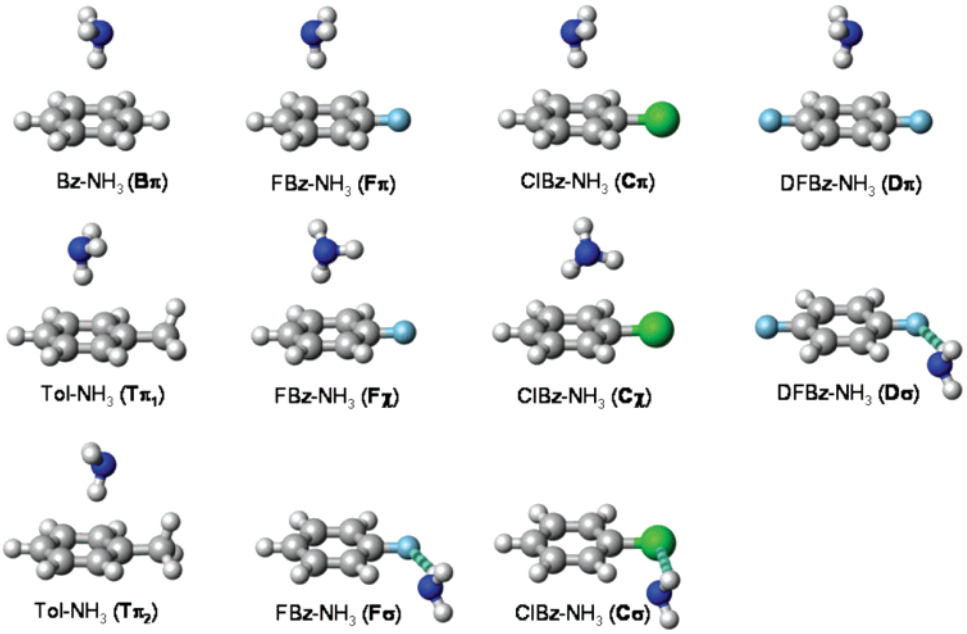

Figure 6. Optimized structures obtained for all the π−**Am** complexes obtained at the RIMP2/aug-cc-pVTZ level.

Table 4. Calculated Interaction Energies, Selected Geometrical Characteristics, and NH Vibrational Frequency Shifts of Various Conformers of All the Aromatic π−**Am** Complexes at the MP2/aug-cc-pVDZ Level of Theory[a]

	Bπ	Tπ_1	Tπ_2	Fπ	Fσ	Fχ	Cπ	Cσ	Cχ	Dπ	Dσ
$-\Delta E^{N}_{e}$	4.45	4.73	5.33	4.27	4.15	4.30	4.53	4.35	4.69	3.75	4.47
$-\Delta E^{B}_{e}$	1.97	2.13	2.69	1.78	2.68	1.81	1.80	2.58	2.01	1.18	2.94
$-\Delta E_{e}$	3.21	3.43	4.01	3.03	3.42	3.06	3.16	3.46	3.35	2.46	3.70
$-\Delta E_{0}$	2.13	2.53	3.04	2.15	2.24	2.18	2.34	2.41	2.39	1.74	2.52
$R_{\pi-H(NH_3)}$	2.362	2.385	2.320	2.477	3.872	2.466	2.506	3.800	2.643	2.366	4.337
$R_{\pi-Hnb(NH_3)}$	3.799	3.722	3.661	3.790	5.023	3.930	3.788	4.916	2.878	3.782	5.368
$R_{\pi-N(NH_3)}$	3.383	3.391	3.261	3.474	4.347	3.446	3.493	4.248	3.204	3.386	4.693
$R_{X-H(NH_3)}$					2.371			2.772			2.413
$R_{X-N(NH_3)}$					2.435			3.646			2.400
$-\Delta\nu_3$	8.4(4)	7.4(4)	10.9(5)	7.1(35)	5.7(6)	7.7(23)	6.5(33)	6.2(7)	12.0(7)	2.4(30)	6.2(7)
$-\Delta\nu_3$	10.8(37)	11.1(39)	18.2(35)	8.0(4)	11.5(17)	9.1(15)	9.9(5)	13.7(19)	22.8(6)	9.2(5)	12.3(15)
$-\Delta\nu_1$	7.5(8)	8.1(8)	13.2(13)	5.9(5)	9.0(10)	6.7(6)	5.5(5)	11.1(11)	16.1(5)	3.1(2)	9.4(8)

[a] $R_{X-H(NH_3)}$ and $R_{X-N(NH_3)}$ are the distances from the fluorine/chlorine atom in fluorobenzene/chlorobenzene to the hydrogen-bonded ammonia hydrogen and ammonia nitrogen, respectively. See footnotes of Table 3, for definitions of other terms.

Table 5. Calculated Interaction Energies and Selected Geometrical Characteristics of Various Conformers of All the Aromatic π−**Am** Complexes at the RIMP2/aug-cc-pVTZ Level of Theory[a]

	Bπ	Tπ_1	Tπ_2	Fπ	Fσ	Fχ	Cπ	Cσ	Cχ	Dπ	Dσ
$-\Delta E^{N}_{e}$	4.59	4.59	5.30	4.45	4.14	4.58	4.66	4.33	4.72	4.19	4.43
$-\Delta E^{B}_{e}$	2.39	2.55	3.00	2.21	2.80	2.21	2.27	2.77	2.50	1.78	3.04
$-\Delta E_{e}$	3.49	3.57	4.15	3.33	3.47	3.39	3.46	3.55	3.61	2.99	3.73
$-\Delta E_{0}$[b]	2.41	2.67	3.21	2.45	2.30	2.52	2.65	2.50	2.65	2.27	2.55
$R_{\pi-H(NH_3)}$	2.370	2.392	2.313	2.484	3.844	2.470	2.513	3.719	2.646	2.376	4.297
$R_{\pi-Hnb(NH_3)}$	3.817	3.759	3.915	3.822	4.991	3.434	3.834	4.867	2.962	3.864	5.326
$R_{\pi-N(NH_3)}$	3.380	3.396	3.260	3.479	4.325	3.366	3.504	4.207	3.255	3.355	4.662
$R_{X-H(NH_3)}$					2.365			2.703			2.403
$R_{X-N(NH_3)}$					3.232			3.595			3.243

[a] See footnotes of Tables 3 and 4, for definitions of various terms. [b] ZPVE corrections were made using the frequencies evaluated at the MP2/aug-cc-pVDZ level.

Benzene/Ammonia and Toluene/Ammonia. The replacement of the olefinic system (ethene) by an aromatic system (**Bz**) (Figure 6) leads to a substantial increase in the magnitude of the interaction energy (Tables 4 and 5). Much of this increase can be attributed to the enhanced dispersion energy in the **Bz**−**Am** complex. At the MP2/aug-cc-pVDZ level, the ZPVE corrected interaction energy (ΔE_0) of the **Bz**−**Am** complex is 2.13 kcal/mol, which is close to the experimental estimate of 1.84 ± 0.12 kcal/mol.[25] An RIMP2/aug-cc-pVQZ optimization of the **Bz**−**Am** complex yielded a BSSE uncorrected interaction energy of 3.05 kcal/mol and a BSSE corrected interaction energy (ΔE^{B}_{e}) of 2.50 kcal/mol. Apart from the fact that the aug-cc-pVQZ optimized geometries exhibit very small BSSE corrections,[78] they are very close to the values obtained at the RIMP2/aug-cc-VTZ level (Table 5). This seems to indicate that the use of the larger aug-cc-pVQZ basis set at the MP2 level would

(77) Sinha, P.; Boesch, S. E.; Gu, C.; Wheeler, R. A.; Wilson, A. K. *J. Phys. Chem. A* **2004**, *108*, 9213.

Table 6. MP2 Equivalent Interaction Energy Components of Some of the Aromatic $\pi-$**Am** and $\pi-H_2O$ Complexes Obtained Using the aug-cc-pVDZ Basis Set[a]

	NH_3											H_2O					
	Bπ	Tπ_1	Tπ_2	Fπ	Fσ	Fχ	Cπ	Cσ	Cχ	Dπ	Dσ	Bπ	Tπ	Fπ	Fσ	Cπ	Cσ
$-E_{int}$[b]	2.03	2.21	2.79	1.85	2.81	1.86	1.88	2.70	2.12	1.29	3.08	2.78	3.25	2.41	3.12	2.51	2.61
$-E_{int}^{(corr)}$[c]	3.35	3.66	3.89	3.33	1.64	3.35	3.61	2.05	4.25	3.43	1.58	2.57	2.91	2.57	1.19	2.84	1.72
$-E_{es}$	2.53	2.72	3.51	2.36	5.02	2.38	2.32	5.09	2.81	1.96	5.41	3.46	4.12	2.99	5.16	3.09	4.54
$-E_{ind}$	1.31	1.43	1.79	1.29	1.60	1.29	1.36	1.88	1.66	1.37	1.74	1.90	2.43	1.81	1.74	1.75	2.19
$-E_{disp}$	4.38	4.75	5.12	4.28	2.82	4.32	4.63	3.29	5.34	4.28	2.86	3.92	4.41	3.77	2.73	4.13	3.09
E_{exch}	6.18	6.70	7.62	6.09	6.63	6.14	6.42	7.56	7.68	6.31	6.94	6.51	7.72	6.16	6.51	6.46	7.20

[a] All energies are in kcal/mol. [b] $E_{int} = E_{es} + E_{ind} + E_{disp} + E_{exch}$. [c] $E_{int}^{(corr)}$ is the sum of all the energy components evaluated at the correlated level.

not dramatically alter the profile of the interaction energies obtained at the MP2/aug-cc-pVTZ level.

A BSSE corrected geometry optimization and vibrational frequency evaluation at the MP2/aug-cc-pVDZ level yields a calculated ZPVE corrected interaction energy of 1.80 kcal/mol for the **Bz**$-$**Am** complex.[79] The calculated $R_{\pi-N(NH_3)}$ (3.629 Å) is also in good agreement with the experimentally determined $R_{\pi-N(NH_3)}$ of 3.590 $\pm$ 0.005 Å.[18,79]As BSSE corrected potential energy surfaces of these $\pi-$**Am** complexes are extremely shallow, geometry convergence involves hundreds of optimization steps. Hence BSSE corrected geometry optimizations have not been carried out for the other complexes because of the enormous computational effort involved.

The MP2/aug-cc-pVDZ shift of the NH stretch ($\nu_1 = -7.5$ cm^{-1}) in the **Bz**$-$**Am** complex (**B**π) is nearly similar to the experimentally observed shift of -8.3 cm^{-1}. Similar to what is observed in the case of the isolated ammonia monomers, small deviations can be noted in the case of ν_3.[73,74,76] The idea that a second σ conformer of **Bz**$-$**Am**[25b] might be responsible for the experimental spectra was ruled out because of its higher energy and the absence of splitting in the ν_3 mode ($\Delta\nu_1 = -5.0$, $\Delta\nu_3 = -6.1, -6.3$ cm^{-1}).[37]

The presence of an electron donating substituent like $-CH_3$ in the π-system (toluene) leads to an asymmetry in the nature of the π-system. As a result, two different conformers are possible in the case of the **Tol**$-$**Am** complex (Figure 6, Table 4). While both conformers **T**π_1 and **T**π_2 exhibit a $\pi-$HN interaction, the latter has an additional weak interaction involving the nitrogen lone pair and the methyl hydrogen. As can be seen from Table 5, the higher interaction energy of conformer **T**π_2 can be attributed to higher contributions from both electrostatic and dispersion energies. The presence of two distinct isomers in the experimental spectra and the significant difference in the calculated interaction energies imply that thermodynamic factors may play a role in conformer stability. Support for the above argument emerges from the fact that the calculated MP2/aug-cc-pVDZ thermal free-energy correction of conformer **T**π_2 is 0.52 kcal/mol larger than that of **T**π_1. While limitations of the theoretical method employed or the basis set used may be responsible for the difference in the interaction energies, it is of interest to note that high-level theoretical investigation of the various conformers of the water hexamer carried out using hexaple zeta basis sets also had to invoke thermodynamic factors to explain the stability of the experimentally observed cage water hexamer.[80]

Based on the calculated vibrational shifts (Table 4), the UV bands 1 and 3 of Figure 3 were tentatively attributed to conformer **T**π_1 and the UV bands 2 and 4, to conformer **T**π_2. The presence of experimental peaks at 49.6 cm^{-1} and 72.7 cm^{-1}, assigned to torsional vibrations in the S_1, which correspond to the calculated numbers for the methyl torsion mode in **T**π_1 (48.7 cm^{-1}) and **T**π_2 (82.6 cm^{-1}) in the S_0 provides additional proof of our conformational assignments. The methyl torsion mode in **T**π_2 appears at high numbers because the weak hydrogen bond between the ammonia nitrogen and the methyl group hydrogen hinders the methyl group rotation.

Halobenzene/Ammonia. As mentioned earlier, the presence of electron-withdrawing substituents such as chlorine or fluorine on the system provides additional avenues for the binding of the ammonia molecule. Thus in the case of the **ClBz**$-$**Am** and **FBz**$-$**Am** complexes, three distinct minimum energy conformers can be identified (Figure 6). Apart from conformers exhibiting a typical π-type of interaction (**C**π and **F**π) or a σ-type of interaction (**C**σ and **F**σ), we also obtain a conformer exhibiting a hybrid $\pi-\sigma$-type of interaction (**C**χ and **F**χ). While a hydrogen bond between the covalently bonded substituent (X = F, Cl) and the ammonia hydrogens is observed in both the σ and χ conformers, its magnitude is much weaker in the case of the latter. It can be seen from Tables 4 and 5 that the interaction energies of all the three conformers are nearly isoenergetic. While calculations at the MP2/aug-cc-pVDZ level indicate that the **C**σ and **F**σ conformers are the lowest energy conformers, those at the RIMP2/aug-cc-pVTZ level indicate that the **C**χ and **F**χ conformers are energetically more stabilized. It might therefore be possible that thermodynamic factors may play an important role in the experimental observation of different conformers. Interestingly at the MP2/aug-cc-pVDZ level, the thermal free-energy correction of the **F**χ conformer is 0.8 kcal/mol smaller than that of the **F**σ conformer. It was shown earlier that the polarizabilities of the system are correlated to the experimental values of $\Delta\nu_1$ in the **ClBz·Am** and **FBz·Am** and **pDFBz·Am** complexes. The nearly similar values of the calculated $\Delta\nu_1$ values in the σ conformers, therefore, make it unlikely that they are responsible for the experimental vibrational spectra in the **ClBz·Am** and **FBz·Am** complexes. Though the interaction energies of both the **C**π and **C**χ conformers are similar (Tables 5 and 6), it can be seen that the experimental shifts are in better agreement with the calculated vibrational shifts of the **C**χ conformer than that of the **C**π conformer. Though the calculated vibrational shifts of both the **F**π and **F**χ conformers seem to be in agreement with the experimental shifts, the latter is more likely the candidate responsible for the experimental spectra.

(78) Lee, E. P. F.; Wright, T. G. *J. Chem. Phys.* **1998**, *109*, 157.
(79) Tarakeshwar, P.; Yang, S.; Kim, K. S.; Kraka, E.; Cremer, D. Unpublished results.
(80) Kim, J.; Kim, K. S. *J. Chem. Phys.* **1998**, 109, 5886.

In the case of the **pDFBz·Am** complex, we obtain only the π bonded **D**π and σ bonded **D**σ conformers. The depleted electron density of the π-system, as a result of the presence of the second fluorine atom, implies that the **D**π conformer is energetically less stabilized than the **D**σ conformer. A comparison of the calculated and experimental vibrational shifts however indicates that the **D**σ conformer gives rise to the experimental spectra. This difference in binding of the **F**χ and **D**σ isomers is in sharp contrast to the isomers of the corresponding π−water complexes.[39a,40b] Therein, the σ conformer (the water molecule forms an H-bond with the covalently bonded fluorine atom) is responsible for the experimental vibrational spectra in the case of both the **FBz**−water and the **DFBz**−water complexes. To rationalize this result, it is useful to examine the salient factors responsible for the stability of the π−**Am** and π−H_2O complexes.

π−Ammonia vs π−Water Complexes. It can be seen from the magnitude of the total interaction energies {E_{int}} in Table 6 that the π−**Am** complexes are less strongly bound than the corresponding π−water complexes. However, the magnitude of $E_{int}^{(corr)}$, which is the sum of all the energy components evaluated at the correlated level, is much higher in the case of the ammonia complexes. Apart from indicating the importance of dispersion energies, this observation also highlights the importance of the inclusion of electron correlation in calculations of these π−**Am** complexes. Given the higher electronegativity of the oxygen atom, the greater interaction energy of the π−water complexes predominantly emerges from the enhanced electrostatic (E_{es}) and induction (E_{ind}) energies. Compared to the π−water complexes, the magnitude of the dispersion (E_{disp}) energies is much higher in the case of the π−**Am** complexes because of the larger polarizability of ammonia (=2.10×10^{-24} cm^3) as compared to water (=1.45×10^{-24} cm^3).

The conformational preference (π, σ, or χ) is governed by both the electron density and the polarizability of the system. Thus the π conformer is not favored in the case of the **DFBz**−**Am** complex because the depleted electron density of *p*-difluorobenzene leads to a smaller electrostatic contribution and its low polarizability ($\alpha = 9.8 \times 10^{-24}$ cm^3) leads to decreased dispersion energies. On the other hand, the considerably higher polarizabilities of the other π-systems lead to higher dispersion energies and hence favor the π or χ conformers.

The π or χ conformers are however not favored in the case of the water complexes, because the increased electronegativity of the oxygen atom would bring the water hydrogen much closer to the π-system (**C**π: $R_{\pi-O} = 3.241$ Å, $R_{\pi-N} = 3.493$ Å) because of enhanced electrostatic energies.[40b] However this closer approach also leads to an increase in the magnitude of the repulsive exchange energies. The above finding clearly establishes that covalently bound halogen substituents apart from influencing the electron density of the system can also synergistically form hydrogen bonds with proton donors.[81] The nature of the proton donor, however, has a significant role in governing the resulting geometry of the complex.

Conclusions

The R2PI spectra of different isomers of clusters of benzene and some of its derivatives with ammonia have been measured in the region of their vibrational origins of the $S_1 \leftarrow S_0$ transition of the clusters. For the **Bz**−**Am** cluster the detailed R2PI spectrum could be assigned by combination of IR/R2PI and IR/UV hole burning spectroscopy. In contrast to previous assignments from the literature only one isomer could be identified for the 1:1 cluster.[25,26b] Other UV bands which have been assigned to different isomers are unambiguously assignable to the 1:2 cluster. Evidence is obtained from the corresponding IR/R2PI spectra in the region of the NH stretches. By high level ab initio calculations, a geometry is found in which the ammonia molecule is located in the center above the benzene ring with one hydrogen atom pointing toward the π-electron system. This so-called π−H-bond was already inferred from microwave spectra.

For the **Tol**−**Am** complex, the R2PI spectrum exhibits four intense absorptions which can be assigned by IR/UV hole burning spectroscopy as bands from two different isomers **T**π_1 and **T**π_2. From ab initio calculations the two isomers are found to be bound via a π-H-bond, similar to the benzene−ammonia. The vibrational spectrum of isomer **T**π_2 shows the same absorption pattern like that of the **Bz**−**Am** cluster with two bands red-shifted relative to the symmetrical and asymmetrical stretching vibrations of the ammonia monomer. In the spectrum of **T**π_1 the vibrational mode in the region of the doubly degenerated asymmetrical vibration is split by 24.2 cm^{-1}. This can be explained by the loss of symmetry in the H-bonded complex. The torsional mode of the methyl group is different in both conformers. There is good correspondence of the measured modes in the S_1 of the conformers with corresponding modes calculated for the S_0.

The spectroscopic analysis of **FBz**−**Am**, **DFBz**−**Am**, and **ClBz**−**Am** indicates that the vibrational spectra of **FBz**−**Am** and **DFBz**−**Am** (Figure 5) are very different. Thus, the latter exhibits a split of the high-frequency mode close to the asymmetric NH-stretching vibration ν_3. This is is contrast to the spectra of **FBz**−water and **DFBz**−water, which were practically the same. The complexes of **FBz**, **ClBz**, and **DFBz** with water are calculated to have the same geometry, with the water molecule lying in the plane of the benzene ring building up a σ-type bond to a halogen atom. With ammonia as the solvent, this σ-type bond is found only for the **DFBz**−**Am** complex. The remaining two exhibit a hybrid χ-type H-bond (π and σ-type bond, see Figure 6). However it is important to mention that all three conformers of **FBz**−**Am** and **ClBz**−**Am** are nearly isoenergetic at the levels of the calculation carried out in this investigation. It might be possible that calculations carried out at higher levels of theory using larger basis sets might be able to unequivocally identify the ultimate isomer structure responsible for the experimental vibrational spectra.

The calculated vibrational spectra are very similar to the experimentally determined ones, thus allowing an analysis of the interaction forces and energies. A detailed decomposition reveals that dispersion energies are the major contributors to the total interaction energies of the π−ammonia complexes. This is in contrast to the corresponding π-complexes with water.

Acknowledgment. B.B. thanks the university Frankfurt and the Fonds der Chemischen Industrie. K.S.K. thanks the Creative

(81) Dunitz, J. D.; Taylor, R. *Chem.−Eur. J.* **1997**, *3*, 89.
(82) Wanna, J.; Menapace, J. A.; Bernstein, E. R. *J. Chem. Phys.* **1986**, *85*, 1795.
(83) Brutschy, B.; Janes, C.; Eggert, J. *Ber. Bunsen-Ges. Phys. Chem.* **1988**, *92*, 74.

Research Initiative Program of the Korean Ministry of Science and Technology {MOST/KOSEF (CRI)} for financial support.

Supporting Information Available: Table S1 containing the magnitudes of the MP2/6-31+G* interaction energies and NH vibrational frequency shifts of all the complexes. Complete refs 57 and 59. This material is available free of charge via the Internet at http://pubs.acs.org.

JA056454J